Romanian Reports in Physics, Vol. 67, No. 4, P. 1261–1270, 2015

Dedicated to
International Year of Light 2015

THEORETICAL INVESTIGATION OF INNER-SHELL PHOTO-IONIZATION X-RAY LASING

V. STĂNCĂLIE, C. IORGA, V. PĂIŞ

National Institute for Laser Plasma and Radiation Physics, Atomistilor 409, P. O. Box MG-36, Magurele-Ilfov, 077125 Romania EU
*Corresponding author *E-mail*: viorica.stancalie@inflpr.ro

Received September 22, 2015

Abstract. Two pumping approaches in which ionization of the lasant is not *via* electron collisions are currently considered for producing x-ray lasers below 100 Å: the field ionization and the inner-shell photo-ionization scheme. Inner-shell photo-ionization x-ray lasers use additional pumping or Auger transitions to selectively populate the upper laser state. We theoretically investigate the inner-shell photo-ionization x-ray lasing for C II using an incoherent x-rays source produced by ultra-short high-intensity laser interaction with ultra thin Cu foil. This work includes structure calculations for neutral, singly and doubly ionized carbon, hydrodynamics of the laser-produced Cu plasma and Non-LTE population kinetics calculations for both the absorber and the lasant material. Competing processes describing the level population distribution include autoionization, Auger decay and collisional ionization of the outer-shell electrons generated during photo-ionization.

Key words: plasma interaction, collisional-radiative model, atomic and ionic spectroscopy.

1. INTRODUCTION

The tremendous progresses made in recent years in the fields of laser-plasma accelerators open the way for the design of compact Free Electron laser that should deliver x-ray beams of 5th generation on the horizon of ten years. In the mid term, the electron beam that is produced with the existing ultra short high intensity (USHI) laser pulses could have an interest for the production of x-rays using Bremsstralhung, Betatron or Compton radiation that are produced respectively when electrons oscillate in the transverse field of the bubble, in slowing down in a high Z material dense target, or when interacting with a laser pulse. Focusing an x-ray free-electron laser beam in an elongated neon-gas target results in a strong exponential amplification of K α fluorescence, as recently demonstrated by N. Rohringer *et al.* [1] and by C. Weninger *et al.* [2].

The recent development of super-intense lasers had led to the discovery of new phenomena in laser interactions with matter. Based on the existing results, the theoretical works entail two directions: to predict new phenomena and interpret the existing observation. The unique opportunities of intensities up to 10^{21} W/cm^2 from a 25 fs laser combined with a high initial contrast of 10^{10} and a repetition rate of 0.1 Hz will allow further studies in advanced laser ion acceleration schemes as well as experiments creating Relativistically Oscillating Mirror (ROM) harmonics. Ion acceleration schemes like Radiation Pressure Acceleration (RPA) or Directed Coulomb Explosion (DCE) will profit from the advantages of a short interaction time of laser and target and high laser energy at the same time, which allows driving those collective acceleration schemes very efficient.

High-resolution spectroscopy in the XUV and x-ray spectral range is used to determine the plasma density, the satellite line emission, or series limits of resonance lines. High resolution K-shell emission in the 1-2 keV energy range from the plasma produced by USHI laser pulses has both the inner-shell x-ray line (K α, K β, L α, etc) as well as ionic x-ray line emission (He α, Ly α) from thermal plasma. The conversion efficiency and the duration of the K α radiation are governed by the generated hot electron spectrum which in turn depends on the laser irradiation parameters as well as the target material. K α emission from USHI pulse laser produced plasmas has been studied by several groups [3–5].

The photo-ionization process in which an electron is energetic enough to be free, *i.e.*, to go into the continuum, represents the background feature of the actually inner-shell photo-pumping scheme. The photo-ionization, also occurs *via* an intermediate doubly excited state which autoionizes when an electron goes free, or can decay by photon emission (dielectronic recombination, DR). The inverse of DR is photo-ionization. The autoionization state introduces resonance in the photo-ionization cross section. In a series of earlier reported works, we have provided atomic data for Li-like and Be-like Al and C ions [6, 7], state selective photo-recombination cross sections [8], autoionization and DR probabilities [9–12] and we theoretically investigated the polarizability of Be-like carbon ion in Rydberg states [13]. The photo-ionization cross sections have been calculated from the generalized line strength using the R-matrix, non-relativistic, semi-relativistic, or full relativistic codes.

In the USHI laser target interaction, the x-ray emission occurs from the high density to over-critical region since the laser energy is deposited during the laser pulse duration which is much shorter than the hydrodynamic time scales of plasma expansion and hence a heated region is created. The self terminating lifetime is not the dominant process that limits the duration of the gain. Instead, the magnitude and duration of the gain is limited by electron collisional ionization of neutral atom. The energetic electrons created in the lasing material by photo-ionization and Auger decay produce predominantly ground state ions that are the lower laser level. The

direct inner shell photo-ionization x-ray pumping scheme requires photon energies at least high enough to photo-ionize the K-shell of lasant material.

A first attempt to theoretically investigate the K α emission from aluminium plasma has been recently reported [14, 15]. In these earlier works we have elucidated the particular feature of the recorded experimental emission spectrum reported at the nhelix test-bed facility at GSI. Our simulation reveals the existence of the K α lines belonging to Al II and Al V ions in a spectrum range of $0.77 - 0.84$ nm where Li-like forbidden and intercombination transitions dominate.

The present paper represents another attempt to improve the theoretical investigation of inner shell photo-ionization x-ray lasing. We refer here to the inner-shell photo-ionization produced as a two step process. The first is to generate hot electrons at the interaction of USHI laser pulse with transition metal elements, as an example. These transition elements have the advantage of 3d open shell. The interaction between the electrons in a high atomic number ion causes the binding energy of the electrons in all shells to depend on each other. Since the electron interaction strength differs between the shells, the energy of the x-ray that results from transitions between different shells also depends on the other electrons, including those in the outer shells that may be ionized away in hot plasma. In the simulation, the multi-terra watt, 35 fs USHI Ti: sapphire source laser at normal incidence on planar copper slab produces a pulse of incoherent x-rays with very rapid rise time. Assuming that a low energy filter removes x-rays that can only ionize outer-shell electrons and the remaining x-rays primary ionize inner-shell electrons of lasant carbon material, we have estimated the initial USHI laser pulse characteristics, the energetic incoherent x-ray flux emerging from the copper slab, and the K-shell spectrum from carbon lasant material. The paper is structured as follows. Section 2 presents the physics models necessary to simulate a multidimensional radiative hydrodynamic problem, including laser-matter interaction, radiation transfer, electron thermal diffusion by conduction, and simple description of non-local thermodynamic equilibrium (NLTE) atomic kinetics. Section 3 gives our conclusions and further direction of research.

2. THEORETICAL MODELS AND SIMULATION RESULTS

We have theoretically investigated K α x-ray line emitted by C^{1+} following an USHI laser pulse at normal incidence on a Cu foil of 200Å layered on a carbon material. The laser parameters have been estimated in such a way that the incoherent x-rays source flux generated during USHI laser interaction with Cu is high enough to rapidly ionize the neutral carbon atom to the K edge yielding K α radiative decay much faster than the other relaxation processes from which Auger decay is dominant. With this respect we have emphasized that the only possible process in the particu-

lar case of B-like C five electron system with a K vacancy and four electrons in the energetically lowest L-shell term, $C^{1+}(1s2s^22p^2\ ^2D,\ ^2P)$, is the direct triple-Auger decay which involves correlated interaction of four electrons. The energy (288 eV) stored in the K-shell excited intermediate $C^{1+}(1s2s^22p^2\ ^2D,\ ^2P)$ state can only produce ionization if the K-shell vacancy is filled by one of the L-shell electrons during the decay processes. The complexity of this four-body process has, very recently, been experimentally reported [16].

In the present calculations we combine hydrodynamics and atomic physics models to model the copper generated plasma including hot electrons fraction and incoherent x-rays source radiation back scattering employing MULTI-fs [17], the full copper plasma emission spectrum *via* FLYCHK [18], the radiative transfer simulation, and the collisional-radiative model for population density distribution over the excited states in carbon within FAC framework [19]. We have simulated dense copper plasma generated at the interaction of a chirped pulse amplification laser system of a Ti:sapphire oscillator and a Ti-sapphire multipass amplifier similar to that described by J. Osterholz *et al.* [20] and M. Cerchez *et al.* [21]. These authors have reported the first experimental investigation of the K-shell emission at the interaction of p-polarized, sub-10-fs laser beam with dense carbon (C) and boron nitride (BN) targets. The laser central wavelength was 790 nm. After compression procedures, the pulse duration of 8 fs has been obtained, with pulse energy on target of 200μJ. The focal spot with 10μm diameter contained 50% of the laser energy resulted in an average intensity in the focal range of 6.5×10^{16} W/cm^2.

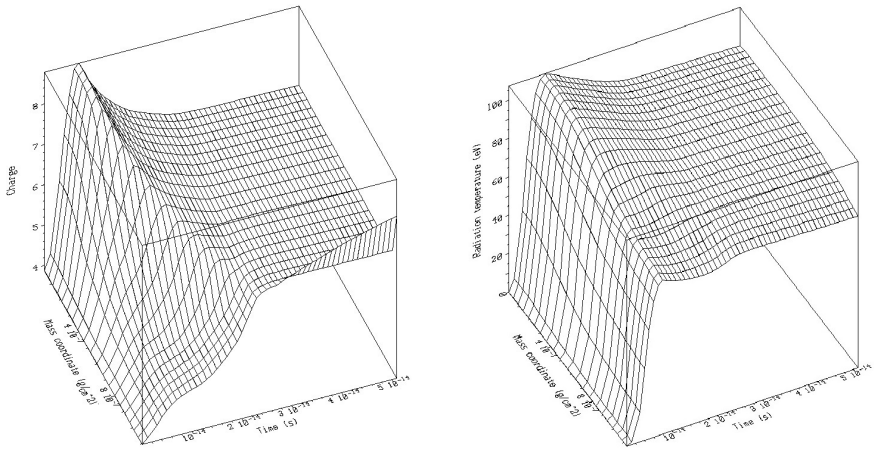

Fig. 1 – The mean ion charge distribution (left) and the radiation field temperature distribution (right) in copper plasma with mass density coordinate (g/cm^2) and plasma expansion time duration (s).

In our simulation, the p-polarized laser beam was at normal incidence onto the

solid, rectangular copper slab of $10\mu m \times 10\mu$m, 200Å thickness, and mass density of 8.96 g/cm^3. The laser deposits energy in the entirety of the copper target due to its reduced thickness as suggested by the simulation. The MULTI-fs code has been successfully used for different fractions of absorbed laser energy f_{th} deposited in a layer with initial thickness of $\delta_0 = 10$Å corresponding to the electron skin depth, and converted into thermal energy of the plasma. The hot electrons component of 1.5% has been considered in this simulation. The simulation results include the laser deposition in the different layers of the target, the time-dependent electron temperature and density along with the radiation temperature and the emitted energy flux. The simulation reveals that the energy deposited in the last layer is more than one order of magnitude lower than the first layer. Figure 1 shows the mean ion charge distribution and the radiation temperature distribution with mass density coordinate (g/cm^2) and plasma expansion time duration (s) in the copper plasma as output from the code.

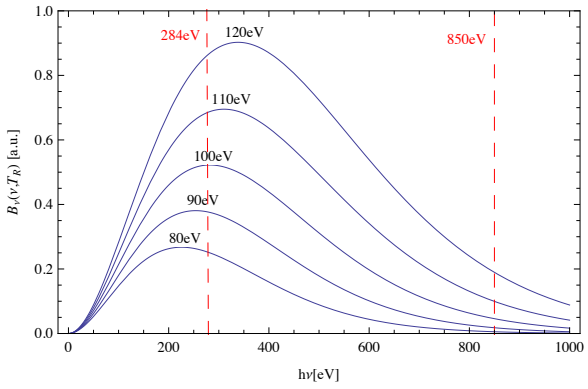

Fig. 2 – Black body radiation for different radiation temperature values given by the hydrodynamic simulations.

The x-ray incoherent pumping field back-scattered from the copper plasma was further modelled to the black body radiation field formula in order to estimate the photon energy range for different radiation temperatures calculated within the hydrodynamic radiation transport MULTI-fs code. Figure 2 shows the spectral distribution of the radiation field.

The time-dependent photon flux emission of the copper plasma is given in Fig. 3. The maximum is attained at $8fs$, then lowers to half of its value at 15 fs and by the time it reaches 50 fs it becomes less than 25% of its initial value. The time integrated rear intensity, $J_{rear} = \int\int I_{rear}(t,\lambda)dtd\lambda$, emitted during the 50 fs time interval within the 284 eV – 850 eV energy range reaches the value of 0.1 J/cm^2. Assuming the rise time of the plasma x-ray radiation field as given by present hydrodynamic simulation, we have filtered the radiative pumping flux (see Fig. 2) in such

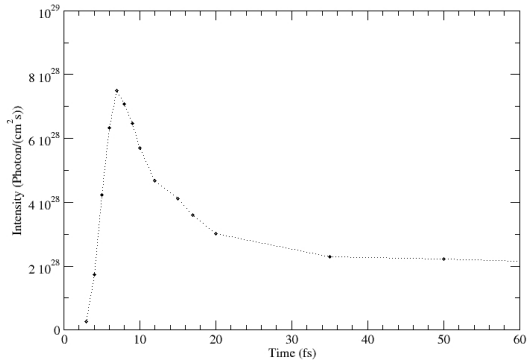

Fig. 3 – Laser-produced copper plasma time-dependent photon flux emission within the $284 - 850$ eV range.

a way the K α emission in carbon takes place before any collisional effects occur and that photo-ionization of the L shell by the filtered x-ray is negligible $(< 5\%)$ [22].

The XUV emission from the expanding plasma was then calculated with time dependent FLYCHK simulations. The code takes into account the line broadening including Stark and Doppler broadening, and opacity effects. The resulted spectrum is plotted in Fig. 4 for particular values of the hot electron component, $f_H = 1.5\%$, and the corresponding temperature, $T_H = 1$ keV.

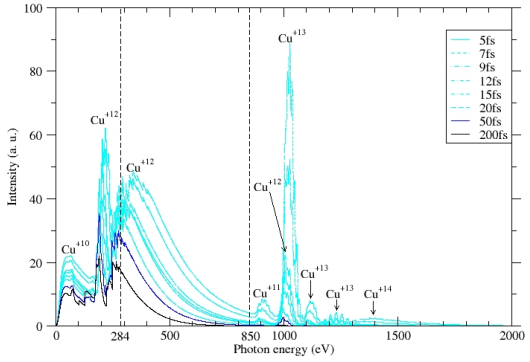

Fig. 4 – Time-dependent synthetic spectrum computed with FLYCHK using the history file obtained from the hydrodynamic simulations.

Finally the x-ray incoherent field source that acts upon the carbon target, has been used as input for atomic kinetics calculation. To do so, we used FAC to describe the population density distribution over the excited states.

Table 1

K-shell hole states belonging to singly ionized carbon

Transition	$h\nu(eV)$ Present work	$h\nu(eV)$ ALS[1]	$h\nu(eV)$ beam-foil[2]	$h\nu(eV)$ dual-plasma[3]	$h\nu(eV)$ R-matrix[4]
$1s2s^22p^2(^2D)$	287.80	287.93	288.68	287.91	287.96
$1s2s^22p^2(^2P)$	287.94	288.40	288.73	288.59	288.63
$1s2s^22p^2(^2S)$	289.25	289.90	290.98	290.53	289.97

[1] Advanced Light Source [23]
[2] Beam-foil experiment [24]
[3] HF +relativistic corrections using Cowan code [25]
[4] R-matrix with radiation damping [23]

In order for the population inversion to take place in the carbon target it is necessary for the x-rays source rise time to be less or equal than the timescale for collisional events, $\tau_{coll} \sim 1/N_{C^0}\sigma_L v$. Here, N_{C^0} is the density for neutral carbon, σ_L is the L-shell electron impact ionization cross section and v is the average electron speed. A great collisional timescale will results in maintaining the population inversion for longer time, but the drawback will consist in a small density of carbon atoms, thus the emitted radiation will become negligible, while on the other hand, if the density is great, the upper lasing level would immediately be depleted and no population inversion would occur. In the case of 50 fs x-ray rise time and assuming a 100 eV value for the electron temperature, the neutral carbon density is restricted to less than 10^{20} cm^{-3} [22].

In the calculation the only ground state of the neutral carbon atom has been included, while singly and doubly ionized carbon ions have been considered with their entire spectrum lines. For singly ionized carbon ion a number of 465 levels have been used in the calculation, whereas for doubly ionized carbon 273 levels have been included. Comparison for C^{1+} K-shell hole state energy levels has been provided in Table 1 with results from [23]. Here, the ALS refers to experiment held at Advanced Light Source synchrotron radiation facility located at the Lawrence Berkeley National Laboratory by A. S. Schlachter $et\ al.$ [23], the beam-foil represents the beam-foil experiment using electron projectile spectroscopy method by M. Rodbro $et\ al.$ [24], the dual plasma refers to the experiment involving two laser-produced plasma by E. Jannitti $et\ al.$ [25]. The processes included in the collisional-radiative coupled rates equations are: the electron collisional excitation and ionization, photo-

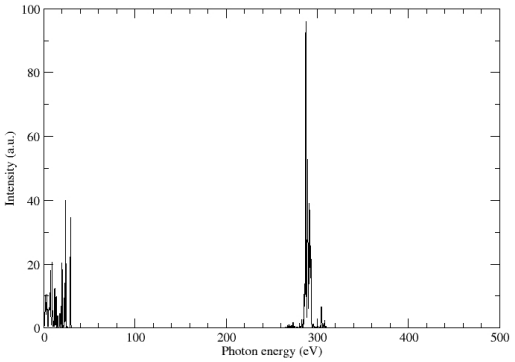

Fig. 5 – Synthetic spectrum resulted from the carbon target irradiated by the copper laser-plasma x-rays source

excitation and photo-ionization, autoionization, Auger decay, radiative decay, three-body recombination, radiative recombination, and dielectronic recombination.

The emission spectrum of the carbon target is plotted in Fig 5. As it was expected, the high-lying C^{1+} states are strongly populated through photo-ionization of neutral carbon states creating a population inversion for the $2p-1s$ lasing transition of 42.99 Å wavelength. The radiative lifetime for the upper level is 293 fs, while the Auger decay channel is dominating having a much lower lifetime of 10.3 fs [22]. The spectrum reveals a strong K α radiation, accounting for more than 60% of the integrated emission spectrum and exceeding 96% of the total emitted energy.

3. CONCLUSION

Inner-shell photo-ionization x-ray lasing in C^{1+} has been simulated for an incoherent x-rays source generated from the USHI laser interaction with Cu absorber. The laser is at normal incident on the front side of the target and the incoherent x-rays source, which pumps the carbon lasant, is due to back-side emission. The simulation was performed using hydrodynamic/atomic codes MULTI-fs/FAC including many physical models treating the radiative hydrodynamic problem, coupled with the NLTE atomic-kinetics models by FLYCHK and the collisional-radiative model (CRM) module from FAC. The simulations give the time-dependent parameters and emission spectrum of the laser-produced Cu plasma and also reveal the temperature, around 105 eV, and the intensity, 2×10^{12} W/cm^2, of the radiation field created by the laser absorber within the representative time period of 50 fs. The incoherent x-rays source creates high populations of inner-shell hole states representing the up-

per levels for the $2p-1s$ lasing transition resulting in K α emission dominating the simulated spectrum. The pursuit of present theoretical studies required new tools of investigation, and in particular laser sources capable of generating such intense fields. Moreover, essential for experiments is not only the super intensity of the laser radiation, but also the extremely short duration of the pulses, of less than 10 femtoseconds, as well as the high repetition rate. On the other hand, the possibility of Laser-Assisted Auger Decay (LAAD) could be checked due to sufficiently intense x-rays field radiation. The idea is to have an inner-shell phenomenon, such as the x-ray photoeffect takes place in an intense optical field, and monitor the changes in the electron energy. This would be expected to appear in the form of ejected electrons with modified energies, due to the absorbed or emitted optical photons. In the present simulation the basic inner-shell effect considered was the Auger emission of electrons: following the creation of a hole in the K-shell of carbon by (low intensity) x-ray photoeffect, a L-shell electron fills the vacancy, while the liberated energy is taken over by another electron from the L-shell, emitted at well defined energy. In order to monitor the modifications due to the applied field, the latter had to be synchronized with the x-ray production of the hole. Theoretical investigation on these effects are in progress.

Acknowledgements. This work is partially supported by the Institute of Atomic Physics under project no. F03. Financial support under the Romanian Space Agency coordinated program STAR Project Number 33 is also acknowledged.

REFERENCES

1. N. Rohringer, D. Ryan, R. A. London, M. Purvis, F. Albert, *et al.*, Nature (London) **481**, 488–491 (2012).
2. C. Weninger, M. Purvis, D. Ryan, R. A. London, J. D. Bozek, C. Bostedt, A. Graf, G. Brown, J. J. Rocca, N. Rohringer, Phys. Rev. Lett. **111**, 233902 (2013).
3. D. Riley, F. Y. Khattak, O. A. M. B. Percie du Sert, R. J. Clarke, E. J. Divali, *et al.*, J. Quant. Spectr. Radiat. Transfer **99**, 537 (2006).
4. J. D. Colvin, K. B. Fournier, J. Kane, S. H. Langer, M. J. May, H. A. Scott, High Energy Density Physics **7(4)**, 263–270 (2011).
5. V. Arora, U. Chakravarty, M. P. Singh, J. A. Chakera, P. A. Naik, P. D. Gupta, Pranama J. Phys. **82**, 365 (2014).
6. V. Stancalie, Physica Scripta **61**, 459–463 (2000).
7. V. Stancalie, Rom. Rep. Phys. **67**, 1087 (2015).
8. V. Stancalie, European J. Phys. D **68(11)**, 349 (2014).
9. V. Stancalie, Laser Part. Beam **31**, 01 (2013).
10. V. Stancalie, Phys. of Plasmas **12**, 043301 (2005).
11. V. Stancalie, Phys. of Plasmas **12**, 100705 (2005).
12. V. Stancalie, NIM B **279**, 147–150 (2012).
13. V. Stancalie, AIP **5**, 077186 (2015).

14. C. Iorga, V. Stancalie, V. Pais, Romanian Reports in Physics (in press).
15. C. Iorga, V. Stancalie, Canadian Journal of Physics DOI:10.1139/cjp-2015-0127 (2015).
16. A. Muller, A. Borovik, J. T. Buhr, J. Hellhund, K. Holste, *et al.*, Phys. Rev. A **114**, 013002 (2015).
17. R. Ramis, K. Eidmann, J. Meyer-Ter-Vehn, S. Huller, Computer Physics Communications **183**, 637–655 (2012).
18. H. K. Chung, M. H. Chen, W. L. Morgan, Y. Ralchenko, R. W. Lee, High Energy Density Physics **1**, 3–12 (2005).
19. M. F. Gu, Can. J. Phys. **86(5)**, 675–689 (2008).
20. J. Osterholz, F. Brandl, T. Fischer, D. Hemmers, M. Cerchez, G. Pretzler, O. Willi, S. J. Rose, Phys. Rev. Lett. **96**, 08502 (2006).
21. M. Cerchez, R. Jung, J. Osterholz, T. Toncian, O. Willi, Phys. Rev. Lett. **100**, 245001 (2008).
22. S. J. Moon, D. C. Eder, Phys. Rev. A **57(2)**, 1391–1394 (1998).
23. A. S. Schlachter, M. M. Sant'Anna, A. M. Covington, A. Aguilar, M. F. Gharaibeh, *et al.*, J. Phys. B: At. Mol. Opt. Phys **37(5)**, L103–L109 (2004).
24. M. Rodbro, R. Bruch, P. Bisgaard, J Phys B: At. Mol. Phys **12**, 2413 (1979).
25. E. Jannitti, M. Gaye, M. Mazzoni, Phys Rev A **47(5)**, 4033 (1993).